

Temperature acclimation in a biochemical model of photosynthesis: a reanalysis of data from 36 species

JENS KATTGE¹ & WOLFGANG KNORR²

¹Max-Planck Institute for Biogeochemistry, Hans-Knöll-Str. 10, 07745 Jena, Germany, ²QUEST, University of Bristol, Department of Earth Sciences, Wills Memorial Building, Queen's Road, BS8 1RJ, UK

ABSTRACT

The Farquhar *et al.* model of C₃ photosynthesis is frequently used to study the effect of global changes on the biosphere. Its two main parameters representing photosynthetic capacity, V_{cmax} and J_{max} , have been observed to acclimate to plant growth temperature for single species, but a general formulation has never been derived. Here, we present a reanalysis of data from 36 plant species to quantify the temperature dependence of V_{cmax} and J_{max} with a focus on plant growth temperature, i.e. the plants' average ambient temperature during the preceding month. The temperature dependence of V_{cmax} and J_{max} within each data set was described very well by a modified Arrhenius function that accounts for a decrease of V_{cmax} and J_{max} at high temperatures. Three parameters were optimized: base rate, activation energy and entropy term. An effect of plant growth temperature on base rate and activation energy could not be observed, but it significantly affected the entropy term. This caused the optimum temperature of V_{cmax} and J_{max} to increase by 0.44 °C and 0.33 °C per 1 °C increase of growth temperature. While the base rate of V_{cmax} and J_{max} seemed not to be affected, the ratio $J_{\text{max}} : V_{\text{cmax}}$ at 25 °C significantly decreased with increasing growth temperature. This moderate temperature acclimation is sufficient to double-modelled photosynthesis at 40 °C, if plants are grown at 25 °C instead of 17 °C.

Key-words: carbon cycle; climate change; Farquhar model; J_{max} ; photosynthetic capacity; V_{cmax} ; V_{max} .

INTRODUCTION

Models to study the impact of global changes on leaves, plants, stands or ecosystems frequently use the biochemical model of C₃ photosynthesis proposed by Farquhar, von Caemmerer & Berry (1980). This model is particularly useful in this context, because it calculates photosynthesis based on a mechanistic representation of the major biochemical processes: carboxylation/oxygenation of ribulose-1,5-bisphosphate (RuBP) by the enzyme ribulose 1,5-bisphosphate carboxylase/oxygenase (Rubisco), and RuBP regeneration.

Correspondence: J. Kattge. Fax: +49 3641 57 7200; e-mail: jkattge@bgc-jena.mpg.de

Most parameters of the Farquhar *et al.* (1980) model are considered to be general for C₃ plants, although they vary to some extent and may acclimate to plant growth conditions (von Caemmerer 2000; Bernacchi, Pimentel & Long 2003; Yamori *et al.* 2006). This variability is assumed to be minor compared to the variability of the two parameters determining photosynthetic capacity: V_{cmax} , carboxylation capacity, and J_{max} , electron transport capacity. These parameters vary by two orders of magnitude and have to be specified for different species and plant growth conditions (Wullschlegel 1993). There is evidence that the temperature dependence of photosynthetic capacity varies with plant growth temperature, which allows plants to perform photosynthesis more efficiently. Many research articles have shown that the electron transport rate adapts to plant growth temperature (for references, see Yamori, Noguchi & Terashima 2005), different configurations of the enzyme Rubisco with different carboxylation characteristics may exist (Yamori *et al.* 2005, 2006) and for single species both parameters, V_{cmax} and J_{max} , have been shown to acclimate to plant growth temperature (Hikosaka, Murakami & Hirose 1999; Medlyn, Loustau & Delzon 2002b; Bernacchi *et al.* 2003; Onoda, Hikosaka & Hirose 2005). But a general formulation of the temperature dependence of V_{cmax} and J_{max} as a function of plant growth temperature has never been quantified for a broader range of species. This is despite the fact that long-term temperature acclimation has become an important issue, as climate models often show rapidly increasing air temperatures within the twenty-first century (Cox *et al.* 2000; Friedlingstein *et al.* 2006), and biosphere model parameters are frequently optimized against eddy covariance data at different sites with different climate regimes (Wang *et al.* 2001, 2007; Braswell *et al.* 2005; Knorr & Kattge 2005).

The response of V_{cmax} and J_{max} to increasing temperature shows a steady rise to an optimum followed by a relatively rapid decline. This response can be modelled by an Arrhenius function modified to account for the decrease of V_{cmax} and J_{max} at high temperatures (Johnson, Eyring & Williams 1942; Medlyn *et al.* 2002a). These functions are based on values of V_{cmax} and J_{max} at a reference temperature of usually 25 °C (V_{cmax}^{25} and J_{max}^{25}). Both V_{cmax}^{25} and J_{max}^{25} show high variation because of species, nutrient availability, season, leaf age and leaf position within the canopy (Medlyn *et al.* 1999; Wilson, Baldocchi & Hanson 2000; Misson *et al.* 2006). For individual species, V_{cmax}^{25} and J_{max}^{25}

may be expected to increase as growth temperature decreases (Yamori *et al.* 2005). In a reanalysis as the one presented, however, with data from several species and experiments, this impact of growth temperature could easily be hidden by large variations of V_{cmax}^{25} and J_{max}^{25} because of other factors (cf. Table 2). Fortunately, the variation in the ratio of J_{max}^{25} to V_{cmax}^{25} is comparatively small and within a range of about one to three, reflecting the coregulation of RuBP carboxylation and regeneration (Wullschlegel 1993; Leuning 1997, 2002; Medlyn *et al.* 1999, 2002a). An impact of plant growth temperature on this balance has been observed in some experiments (Hikosaka *et al.* 1999; Onoda *et al.* 2005; Yamori *et al.* 2005), but was absent in others (Bunce 2000; Medlyn *et al.* 2002b). The activation energy and the optimum temperature of V_{cmax} and J_{max} have been observed to be positively related to plant growth temperature for single cases (Hikosaka *et al.* 1999; Medlyn *et al.* 2002b; Bernacchi *et al.* 2003; Onoda *et al.* 2005), but this still needs to be confirmed for a broader range of species.

We here present a reanalysis of the temperature dependency of V_{cmax} and J_{max} in the context of one consistent parameterization of the Farquhar *et al.* (1980) model for 36 species, a considerably broader range than has previously been analysed. This reanalysis is based on the review by Medlyn *et al.* (2002a), but the broader range of data sets may enable us to find general relationships between plant growth temperature and the temperature dependence of V_{cmax} and J_{max} . In contrast to Leuning (2002), all data sets are standardized to one consistent parameterization of the Farquhar *et al.* (1980) model. This is essential when comparing results from different experiments (Medlyn *et al.* 2002a). Based on the results of our reanalysis, we will discuss the consequences of the observed relationships for modelled photosynthesis rates in a global context, such as for simulations of the interaction between the terrestrial biosphere and climate change for the next 100 years (Cox *et al.* 2000; Friedlingstein *et al.* 2006).

METHODS

Photosynthesis model

Several formulations and parameterizations of the original model by Farquhar *et al.* (1980) have been described. Here, we refer to the formulation and parameterization used by Medlyn *et al.* (2002a) using the formulation of Rubisco kinetics proposed by Bernacchi *et al.* (2001).

Temperature dependence of V_{cmax} and J_{max}

We use the following modified Arrhenius function (Johnson *et al.* 1942) to describe the temperature dependence of V_{cmax} and J_{max} :

$$k_T = k_{25} \exp[H_a(T_1 - T_{\text{ref}})/(T_{\text{ref}}RT_1)] \frac{1 + \exp\left(\frac{T_{\text{ref}}\Delta S - H_d}{T_{\text{ref}}R}\right)}{1 + \exp\left(\frac{T_1\Delta S - H_d}{T_1R}\right)} \quad (1)$$

This function refers to the base rate of V_{cmax} and J_{max} at reference temperature of 25 °C, denoted k_{25} . H_a is the activation energy, H_d is the deactivation energy, which describes the rate of decrease above the optimum temperature, and ΔS is the so-called entropy factor. T_1 , leaf temperature, and T_{ref} , reference temperature, are given in Kelvin. If all four parameters are allowed to vary during optimization, the model tends to be underdetermined by given measurements. This is because of a high correlation among parameters determining the deactivation of V_{cmax} and J_{max} , namely H_d and ΔS , so that results are difficult to compare. Because H_d is in most cases found to be close to 200 kJ mol⁻¹ (Medlyn *et al.* 2002a), we fixed H_d to 200 kJ mol⁻¹ and thus reduced the number of free parameters of the temperature function to three: k_{25} , ΔS and H_a .

The optimum temperatures of V_{cmax} and J_{max} , T_{opt} (also in K) can be derived from the function mentioned earlier (Medlyn *et al.* 2002b):

$$T_{\text{opt}} = \frac{H_d}{\Delta S - R \ln\left(\frac{H_a}{H_d - H_a}\right)} \quad (2)$$

Finally, the base rate of J_{max} , J_{max}^{25} was assumed to be related to the base rate of V_{cmax} , V_{cmax}^{25} , through:

$$J_{\text{max}}^{25} = r_{J,V} \times V_{\text{cmax}}^{25} \quad (3)$$

Temperature acclimation of V_{cmax} and J_{max}

We sought to derive linear relationships between plant growth temperature, t_{growth} (in °C), and the three free parameters of Eqn 1 (base rate, k_{25} , activation energy, H_a and entropy term, ΔS), as well as optimum temperature, T_{opt} and the ratio of $J_{\text{max}}^{25}/V_{\text{cmax}}^{25}$, $r_{J,V}$, using a general formulation described by:

$$x_i = a_i + b_i \times t_{\text{growth}} \quad (4)$$

where the acclimation parameters a_i and b_i are derived for each parameter x_i representing k_{25} , H_a , ΔS , T_{opt} and $r_{J,V}$.

Data

The compilation of data contains values of V_{cmax} and J_{max} for 36 species – summarizing groups in Wohlfahrt *et al.* (1999) – covering broadleaved trees and shrubs, needle-leaved (coniferous) trees, grasses and other herbaceous plants. Measurements were taken at temperatures varying from 5 to 40 °C. Growth temperatures, defined as the average of day and night temperature from the preceding month (Medlyn *et al.* 2002a), varied between 11 and 35 °C. An overview of the sources of the data compilation is given in Table 1.

The original values of the data used in this compilation had been derived by inversion of the Farquhar *et al.* (1980) photosynthesis model, fitting V_{cmax} and J_{max} against gas-exchange measurements taken on single leaves. This

Table 1. Details of data sets used

Species	Reference	Growth conditions	t_{growth}	Points	t_{min}	t_{max}	Notes
Broadleaved trees and shrubs							
<i>Acer pseudoplatanus</i>	Dreyer <i>et al.</i> (2001)	N (France)	16	26	10	40	(1)
<i>Aristotelia serrata</i>	Dungan, Whitehead & Duncan (2003)	GH (NZ)	14	17	10	30	
<i>Betula pendula</i>	Dreyer <i>et al.</i> (2001)	N (France)	17	19	10	40	(1)
<i>B. pendula</i>	Wang (unpublished results)	OTC (Finland)	14	20	5	32	(2)
Dwarf shrub	Wohlfahrt <i>et al.</i> (1999)	Field (Austria)	11	8	5	40	
<i>Eucalyptus pauciflora</i>	Kirschbaum & Farquhar (1984)	GH-T	20		15	35	(2)
<i>Fagus crenata</i>	Onoda <i>et al.</i> (2005)	N (Japan)	13, 16, 25	18	10	35	
<i>Fagus sylvatica</i>	Dreyer <i>et al.</i> (2001)	N (France)	17	19	10	40	(1)
<i>F. sylvatica</i>	Strassemeyer & Forstreuther (1997)	ME (Germany)	20	28	19	35	(2)
<i>Fraxinus excelsior</i>	Dreyer <i>et al.</i> (2001)	N (France)	16	27	10	40	(1)
<i>Fuchsia excorticata</i>	Dungan <i>et al.</i> (2003)	GH (NZ)	14	18	10	30	
<i>Juglans regia</i>	Dreyer <i>et al.</i> (2001)	N (France)	17	22	10	40	(1)
<i>Prunus persica</i>	Walcroft <i>et al.</i> (2002)	N (France)	19	19	12	37	(2)
<i>Quercus petraea</i>	Dreyer <i>et al.</i> (2001)	N (France)	16	22	10	40	(1)
<i>Quercus robur</i>	Dreyer <i>et al.</i> (2001)	N (France)	16	28	10	40	(1)
<i>Q. robur</i>	Strassemeyer & Forstreuther (unpublished results)	ME (Germany)	20	29	15	36	(2)
Coniferous trees							
<i>Abies alba</i>	Robakowski, Montpied & Dreyer (2002)	N (France)	25	28	10	40	(1,2)
<i>Pinus densiflora</i>	Han <i>et al.</i> (2004)	Field (Japan)	15, 21	5	12	33	
<i>Pinus pinaster</i>	Medlyn <i>et al.</i> (2002a)	Field (France)	24	27	15	35	
<i>Pinus radiata</i>	Walcroft & Kelliher (1997)	GH (NZ)	24	14	8	30	(2)
<i>Pinus sylvestris</i>	Wang, Kellomaki & Laitinen (1996)	OTC (Finland)	14	5	6	32	(2)
<i>Pinus taeda</i>	Ellsworth & Klimas (unpublished)	FACE (N. Carolina)	24	18	15	35	(2)
Herbaceous plants							
<i>Abutilon theophrasti</i>	Bunce (2000)	GH-T	15, 25	5	15	35	
<i>Brassica rapa</i>	Bunce (2000)	GH-T	15, 25	5	15	35	
<i>Chenopodium album</i>	Bunce (2000)	GH-T	15, 25	5	15	35	
Forbs, abandoned area	Wohlfahrt <i>et al.</i> (1999)	Field (Austria)	11	8	5	40	
Forbs, meadow	Wohlfahrt <i>et al.</i> (1999)	Field (Austria)	11	8	5	40	
Forbs, pasture	Wohlfahrt <i>et al.</i> (1999)	Field (Austria)	11	8	5	40	
<i>Glycine max</i>	Bunce (2000)	GH-T	15, 25	5	15	35	
<i>Glycine max</i>	Harley, Weber & Gates (1985)	GH-T	25	48	20	40	(2)
<i>Gossypium hirsutum</i>	Harley <i>et al.</i> (1992)	GH-T	29	16	18	33	(2)
Graminoid, abandoned area	Wohlfahrt <i>et al.</i> (1999)	Field (Austria)	11	8	5	40	
Graminoid, meadow	Wohlfahrt <i>et al.</i> (1999)	Field (Austria)	11	8	5	40	
Graminoid, pasture	Wohlfahrt <i>et al.</i> (1999)	Field (Austria)	11	8	5	40	
<i>Helianthus annuus</i>	Bunce (2000)	GH-T	15, 25	5	15	35	
<i>Hordeum vulgare</i>	Bunce (2000)	GH-T	15, 25	5	15	35	
<i>Lycopersicon esculentum</i>	Bunce (2000)	GH-T	15, 25	5	15	35	
<i>Nicotiana tabacum</i>	Bernacchi <i>et al.</i> (2003)	GH-T	14, 25, 35	7	10	40	
<i>Polygonum cuspidatum</i>	Onoda <i>et al.</i> (2005)	N (Japan)	13, 16, 25	18	10	35	
<i>Vicia faba</i>	Bunce (2000)	GH-T	15, 25	5	15	35	

Notes: (1) One night acclimation to measurement temperature; (2) data sets as published by Medlyn *et al.* (2002a).

t_{growth} , growth temperature; t_{min} , minimum measurement temperature in Celsius; t_{max} , maximum measurement temperature in Celsius; Points, number of data points; N, nursery; GH, greenhouse; GH-T, greenhouse temperature controlled; OTC, open-top chamber experiment; ME, mini-ecosystem experiment; FACE, free-air carbon-enrichment experiment.

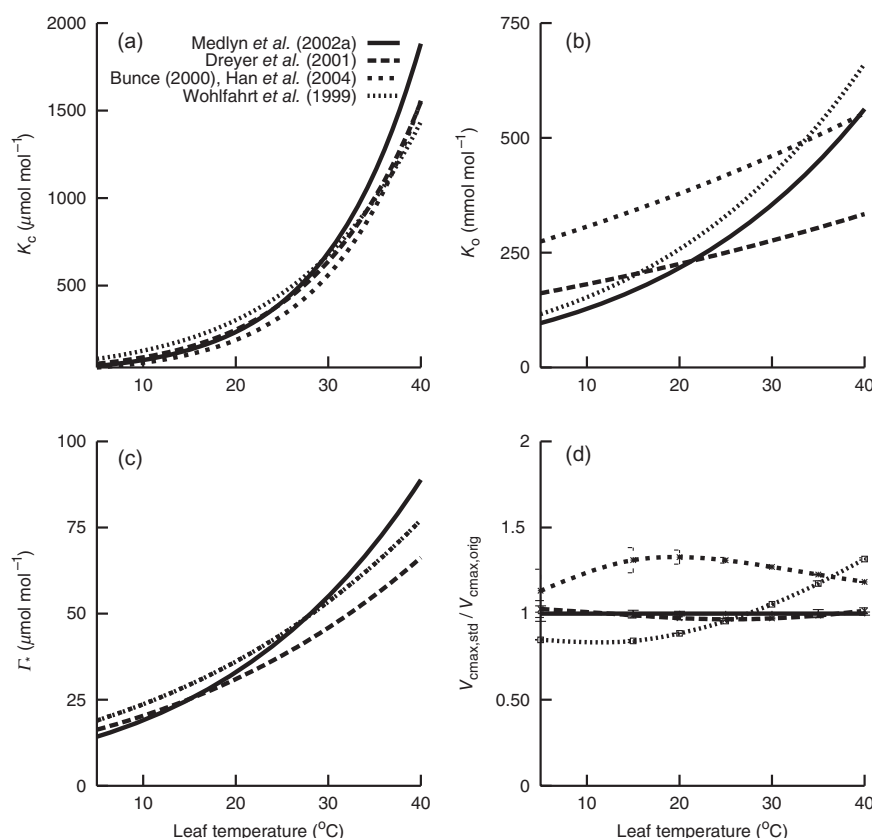


Figure 1. (a–c) Temperature dependence of K_c , K_o and Γ^* used by various studies. (d) Ratio of standardized to published values of V_{cmax} for the same studies. The error bars indicate the SE caused by inversion of standardized V_{cmax} against recalculated photosynthesis rates.

approach has the advantage that measurements are performed *in vivo*, thus the derived model parameters characterize photosynthetic performance of intact leaves. However, the values of V_{cmax} and J_{max} are thus not independent of the values of other model parameters describing Rubisco kinetics (Fig. 1a–c) and light conversion. As a consequence, values of V_{cmax} and J_{max} derived with different model parameterizations are not directly comparable (Medlyn et al. 2002a), and the published values of V_{cmax} and J_{max} had to be standardized to one consistent formulation and parameterization. We took the published value of V_{cmax} and the published parameterization of Γ^* , K_c , K_o at the given temperature to compute A_c for $O_i = 0.21$ mol (O_2)/mol (air) and $C_i = 50, 100, 150, 200$ and 250 ppm. These $A_c - C_i$ curves from pseudo-measurements were then used to obtain standardized values of V_{cmax} by model fitting based on the parameters used here. The corresponding correction functions are shown in Fig. 1d. To standardize J_{max} , we used the published light conversion equation (giving J as a function of Q) and given irradiance Q to calculate the electron flux, J , from the published value of J_{max} . Using the published temperature dependence of Γ^* , and $C_i = 0.85C_a$, (C_a : atmospheric CO_2 concentration given in the publication), we calculated A_j . These pseudo-fluxes were then used to derive standardized values of J_{max} . These procedures were applied to data from Wohlfahrt et al. (1999), Bunce (2000), Dreyer et al. (2001), Bernacchi et al. (2003) and Han et al. (2004). We tested our correction procedure against parameter values directly derived from original

measurements by Medlyn et al. (2002a) for several data sets (Harley et al. 1992; Walcroft & Kelliher 1997; Dreyer et al. 2001; Walcroft et al. 2002). The differences between our corrected values and those of Medlyn et al. (2002a) were in a reasonably small range. While the correction of V_{cmax} was quite significant, the correction of J_{max} was small in all cases: the ratio of standardized to published values for J_{max} was between 0.95 and 1.05.

Following this standardization, the compilation was consistent with respect to measurement technique and model parameterization, retaining differences between plant species, plant growth environment and treatment before measurement. Different plant species were classified into broadleaved trees, coniferous trees and herbaceous plants. The growth environment was characterized either by controlled or by naturally variable temperature regime. In general, no special treatment was applied before measurement and only single leaves were exposed to the measurement temperature, while the plants were kept within their growth environments. In two cases, however, (Dreyer et al. 2001; Robakowski et al. 2002), the whole plant was taken from its growth environment into climate chambers and exposed to the respective measurement temperature 1 d (24 h) in advance. For example, before gas-exchange measurements at 40°C were conducted to determine V_{cmax} and J_{max} at 40°C leaf temperature plants were exposed to 40°C for 24 h; before measurements at 25°C , plants were exposed to 25°C for 24 h. Those data were separated (for reasons of 'pretreatment'), because an acclimation to the

respective measurement temperature may already have occurred at the time of measurement (Yamori *et al.* 2005, 2006).

Models of temperature dependence fitted against individual data sets

To analyse the temperature dependence of V_{cmax} and J_{max} , the temperature functions were optimized against each data set using the Marquardt–Levenberg algorithm (Levenberg 1944), weighting all points equally. The temperature functions with three free parameters, k_{25} , H_a and ΔS , were able to fit the data very well, as indicated by an average explained variance (r^2) of 0.960 and 0.917 for V_{cmax} and J_{max} , respectively (Table 2).

Deriving average models with and without temperature acclimation

We derived two generalized models each to describe the temperature dependence of V_{cmax} and J_{max} from the individually fitted measurements. One general formulation is the average model without temperature acclimation, which is simply derived by averaging the parameter values across individual measurements. The other general model includes temperature acclimation and was derived by computing a linear regression of individually fitted values of k_{25} , H_a , ΔS and $r_{\text{J,V}}$ against plant growth temperature (see Eqn 4).

The results are based on all data sets, except for those that had undergone ‘pretreatment’ and those with optimum temperatures of V_{cmax} above 50 °C (two cases) or J_{max} below 20 °C (two cases). Optimum temperatures above 50 °C were supposed to be too high above their highest measurement temperatures to derive reliable estimates of ΔS and T_{opt} . Optimum temperatures below 20 °C were assumed to be exceptionally low, with a high risk of measurement errors. Data sets used to derive the average models and temperature acclimation are indicated in Table 2.

Comparison of derived temperature functions

It is the objective of this analysis to find a general functional form for the temperature dependence of both V_{cmax} and J_{max} that can be used in global and large-scale modelling studies. This general functional form to characterize the temperature dependence without temperature acclimation can be written as:

$$\begin{aligned} V_{\text{cmax}}(T_1) &= V_{\text{cmax}}^{25} f(T_1) \\ J_{\text{max}}(T_1) &= V_{\text{cmax}}^{25} r_{\text{J,V}} g(T_1) \end{aligned} \quad (5)$$

Thus, a global model will only require one plant-type specific parameter, V_{cmax}^{25} . $f(T_1)$ and $g(T_1)$ correspond to Eqn 1 with k_{25} replaced by 1. The functions f and $r_{\text{J,V}}g$ are considered the normalized temperature functions of V_{cmax} and J_{max} , and they are also used to characterize the

individually fitted functions divided by V_{cmax}^{25} , which are marked by a subscript denoting the individual fit: $f_i(T_1)$ and $r_{\text{J,V},i}g_i(T_1)$.

We use the root mean square error (RMSE) to characterize the mismatch of the general normalized temperature functions, $f(T_1)$ and $r_{\text{J,V}}g(T_1)$, against the individual temperature functions, $f_i(T_1)$ and $r_{\text{J,V},i}g_i(T_1)$. Thus, for the temperature models of V_{cmax} and J_{max} without acclimation, the RMSE is given by:

$$\begin{aligned} \text{RMSE}_V(T_1) &= \sqrt{\frac{1}{n} \sum_{i=1}^n [f(T_1) - f_i(T_1)]^2} \\ \text{RMSE}_J(T_1) &= \sqrt{\frac{1}{n} \sum_{i=1}^n [r_{\text{J,V}}g(T_1) - r_{\text{J,V},i}g_i(T_1)]^2} \end{aligned} \quad (6)$$

where the index, i , runs over the individually fitted temperature functions considered.

For the temperature model with acclimation, f and $r_{\text{J,V}}g$ still have one general functional form to be used globally, but also contain a parameter that is specific for each data set, the growth temperature, t_{growth} .

$$\begin{aligned} V_{\text{cmax}}(T_1) &= V_{\text{cmax}}^{25} f(T_1; t_{\text{growth}}) \\ J_{\text{max}}(T_1) &= V_{\text{cmax}}^{25} r_{\text{J,V}}(t_{\text{growth}}) g(T_1; t_{\text{growth}}) \end{aligned} \quad (7)$$

Thus, for the model with acclimation, RMSE for V_{cmax} and J_{max} is given as

$$\begin{aligned} \text{RMSE}_V(T_1) &= \sqrt{\frac{1}{n} \sum_{i=1}^n [f(T_1; t_{\text{growth},i}) - f_i(T_1)]^2} \\ \text{RMSE}_J(T_1) &= \sqrt{\frac{1}{n} \sum_{i=1}^n [r_{\text{J,V}}(t_{\text{growth},i}) g(T_1; t_{\text{growth},i}) - r_{\text{J,V},i}g_i(T_1)]^2} \end{aligned} \quad (8)$$

where $t_{\text{growth},i}$ is the growth temperature that belongs to each specific data set.

RESULTS

Impact of plant type and growth environment on individually fitted parameters

An impact of plant type on individually fitted parameters was only apparent in case of the base rates V_{cmax}^{25} and J_{max}^{25} , as the average values of broadleaved and coniferous plants were about half the average of herbaceous plants (Fig. 2a,b), and for the activation energy, H_a , of V_{cmax} . In the latter case, two herbaceous outliers to high values could be observed (Fig. 2c). An impact of controlled versus natural growth environment was not observed.

Impact of plant growth temperature on individually fitted parameters

The individually fitted values for V_{cmax}^{25} and J_{max}^{25} varied by a factor of five to six, but did not show any impact of plant growth temperature. The slopes of their temperature acclimation functions (Eqn 4) were slightly positive, but not

Table 2. Parameter values to characterize the temperature response of V_{cmax} and J_{max} for individually fitted data sets

Species	t_{growth} (°C)		V_{cmax}		H_{a}		H_{d}		ΔS		r^2	t_{opt} (°C)
			V_{cmax}^{25} ($\mu\text{mol m}^{-2} \text{ s}^{-1}$)	SE	(J mol^{-1})	SE	(J mol^{-1})	($\text{J mol}^{-1} \text{ }^{\circ}\text{C}^{-1}$)	SE			
Broadleaved trees and shrubs												
<i>Acer pseudoplatanus</i>	16	26	78.2	6.9	84 917	22 030	200 000	648.2	5.6	0.810	34.3	
<i>Aristotelia serrata</i>	14	17	37.8	3.6	60 176	19 580	200 000	653.3	9.4	0.746	29.9	
<i>Betula pendula</i>	17	19	68.3	4.6	67 119	9857	200 000	633.6	4.0	0.952	39.8	
<i>B. pendula</i> OTC	14	20	101.9	3.9	63 750	11 440	200 000	655.3		0.970	29.3	
Dwarf shrub	11	8	33.6	0.5	78 051	3209	200 000	649.4	0.9	0.998	33.2	
<i>Eucalyptus pauciflora</i>	20		90.4	0.0	60 790	4930	200 000	636.5		1.000	37.8	
<i>Fagus crenata</i>	13	18	17.3									
<i>F. crenata</i>	16	18	24.7									
<i>F. crenata</i>	25	18	25.7									
<i>Fagus sylvatica</i>	17	19	62.8	3.7	70 627	9576	200 000	638.4	3.1	0.949	37.8	
<i>F. sylvatica</i> ME	20	28	27.5	2.9	65 400	19 480	200 000	640.9		0.950	36.2	
<i>Fraxinus excelsior</i>	16	27	76.3	5.8	51 778	8699	200 000	618.9	15.1	0.895	45.6	
<i>Fuchsia excorticata</i>	14	18	77.1	8.6	72 480	33 370	200 000	662.8	10.3	0.520	26.6	
<i>Juglans regia</i>	17	22	62.3	2.7	109 327	12 400	200 000	648.6	2.8	0.975	36.1	
<i>Prunus persica</i>	19	19	66.2	3.9	75 140	2338	200 000	613.3		0.990	50.9	
<i>Quercus petrea</i>	16	22	86.9	3.1	57 235	4023	200 000	624.1	4.0	0.984	43.6	
<i>Quercus robur</i>	16	28	95.1	4.7	55 729	5868	200 000	628.4	4.2	0.949	41.3	
<i>Q. robur</i> ME	20	29	42.3	13.4	57 590	12 220	200 000	634.0		0.970	38.8	
Coniferous trees												
<i>Abies alba</i>	25	28	43.5	5.3	60 020	9880	200 000	638.5		0.950	36.8	
<i>Pinus densiflora</i>	15	5	64.8	0.3	63 967	1070	200 000	660.5	0.3	1.000	27.0	
<i>P. densiflora</i>	21	5	51.8	0.5	74 919	2964	200 000	648.6	0.9	0.999	33.3	
<i>P. densiflora</i>	15	5	61.5	4.2	77 735	27 040	200 000	666.0	6.9	0.936	25.6	
<i>Pinus pinaster</i>	24	27	92.4	4.7	74 160	11 170	200 000	638.0		0.990	38.3	
<i>Pinus radiata</i>	24	14	85.9	17.7	64 780	21 320	200 000	637.4		0.980	37.7	
<i>P. radiata</i>	24	14	99.2	4.7	51 320	19 210	200 000	634.8		0.960	37.7	
<i>Pinus sylvestris</i>	14	18	67.3	9.7	69 830	12 560	200 000	660.2		0.960	27.6	
<i>Pinus taeda</i>	24	14	57.7	9.4	61 210	304	200 000	606.1		0.980	53.3	
Herbaceous plants												
<i>Abutilon theophrasti</i>	15	5	157.5	4.1	55 848	5551	200 000	646.2	2.2	0.994	32.8	
<i>A. theophrasti</i>	25	5	170.8	7.1	63 861	9166	200 000	645.4	3.6	0.990	33.9	
<i>Brassica rapa</i>	15	5	187.1	1.4	54 373	1642	200 000	648.3	0.6	0.999	31.6	
<i>B. rapa</i>	25	5	127.1	2.7	65 493	4799	200 000	647.0	1.7	0.997	33.3	
<i>Chenopodium album</i>	15	5	196.6	9.0	63 539	10 430	200 000	647.5	3.7	0.985	32.9	
<i>C. album</i>	25	5	162.1	5.2	70 729	7305	200 000	642.6	3.3	0.996	35.8	
Forbs abandoned area	11	8	50.2	1.1	70 277	4183	200 000	656.3	1.2	0.996	29.4	
Forbs meadow	11	8	77.0	1.0	73 336	2723	200 000	653.7	0.8	0.998	30.8	
Forbs pasture	11	8	67.8	1.8	73 544	5391	200 000	653.0	1.5	0.994	31.2	
<i>Glycine max</i>	15	5	130.2	17.6	85 880	44 820	200 000	657.2	11.0	0.896	30.2	
<i>G. max</i>	25	5	152.8	3.2	45 371	4024	200 000	641.8	2.3	0.995	33.8	
<i>G. max</i>	25	48	93.9	8.3	69 500	24 370	200 000	629.9		0.880	41.9	
<i>Gossypium hirsutum</i>	29	16	90.2		116 380		200 000	646.7		1.000	40.6	
Graminoid abandoned area	11	8	49.2	0.8	59 321	2667	200 000	650.4	0.9	0.997	31.1	
Graminoid meadow	11	8	53.8	1.8	84 801	8141	200 000	656.1	2.1	0.993	30.6	
Graminoid pasture	11	8	57.2	1.6	172 838	5883	200 000	666.9	1.7	0.999	34.0	
<i>Helianthus annuus</i>	15	5	186.0	3.4	64 868	4174	200 000	648.3	1.4	0.998	32.6	
<i>H. annuus</i>	25	5	192.6	6.4	63 980	7618	200 000	648.0	2.7	0.992	32.7	
<i>Hordeum vulgare</i>	15	5	200.7	9.1	67 418	11 850	200 000	654.2	3.3	0.980	30.1	
<i>H. vulgare</i>	25	5	165.0	2.6	62 568	3388	200 000	643.9	1.5	0.999	34.5	
<i>Lycopersicon esculentum</i>	15	5	123.1	2.2	73 018	4495	200 000	649.9	1.4	0.998	32.6	
<i>L. esculentum</i>	25	5	128.2	1.4	65 756	2456	200 000	646.0	0.9	0.999	33.8	
<i>Nicotiana tabacum</i>	14	7										
<i>N. tabacum</i>	25	7										
<i>N. tabacum</i>	35	7										
<i>Polygonum cuspidatum</i>	13	18	45.7									
<i>P. cuspidatum</i>	16	18	38.3									
<i>P. cuspidatum</i>	25	18	50.9									
<i>Vicia faba</i>	15	5	205.2	4.8	83 500	7590	200 000	657.0	1.9	0.996	30.1	
<i>V. faba</i>	25	5	174.4	4.6	76 322	7219	200 000	652.5	2.0	0.995	31.7	

Data sets excluded from the different analyses are marked in columns named 1–3.

1, Data sets excluded from the analysis of the temperature dependence of V_{cmax} because of pretreatment or optimum temperatures above 50 °C.

2, Data sets excluded from the analysis of the temperature dependence of J_{max} because of pretreatment or optimum temperatures below 20 °C.

3, Data sets excluded from the analysis of the temperature dependence of $J_{\text{max}}^{25}/V_{\text{cmax}}^{25}$ because of pretreatment or optimum temperatures below 20 °C.

J_{\max}												
J_{\max}^{25} ($\mu\text{mol m}^{-2} \text{s}^{-1}$)	SE	H_a (J mol^{-1})	SE	H_d (J mol^{-1})	ΔS ($\text{J mol}^{-1} \text{ } ^\circ\text{C}^{-1}$)	SE	r^2	T_{opt} ($^\circ\text{C}$)	r_{LV}	1	2	3
148.7	8.2	46 083	8656	200 000	645.4	3.1	0.747	32.1	1.90	×	×	×
78.6	6.7	52 304	15 500	200 000	648.8	11.2	0.784	31.2	2.08			
119.8	3.2	40 589	3467	200 000	635.1	1.7	0.956	36.4	1.75	×	×	×
111.9	1.5						0.960	19.2	1.10		×	×
72.4	6.4	66 873	17 100	200 000	656.2	5.0	0.935	29.1	2.16			
141.9	0.0	43 790		200 000	644.8			32.2	1.57			
47.1									2.72			
51.4									2.08			
54.9									2.14			
119.5	4.6	53 519	6033	200 000	640.1	2.1	0.934	35.4	1.90	×	×	×
44.8	7.5	43 360	12 370	200 000	647.7		0.940	30.8	1.63			
146.3	5.7	48 652	6252	200 000	642.5	2.2	0.873	33.8	1.92	×	×	×
152.3	15.8	42 490	18 700	200 000	650.6	13.6	0.498	29.3	1.97			
108.2	3.1	60 224	4892	200 000	641.2	1.6	0.959	35.5	1.74	×	×	×
106.5	9.3	49 984	19 200	200 000	639.0	8.8	0.956	35.6	1.61	×		
158.5	3.4	48 154	2765	200 000	635.3	1.3	0.981	37.1	1.82	×	×	×
157.5	6.6	40 719	4916	200 000	632.1	3.3	0.891	37.8	1.66	×	×	×
66.0	20.2	35 870	13 520	200 000	641.3		0.890	32.9	1.56			
95.5	5.7	50 820	8200	200 000	644.2		0.900	33.2	2.20	×	×	×
155.8	1.3	61 198	1794	200 000	649.0	0.8	1.000	32.0	2.40			
78.4	1.4	77 971	5379	200 000	649.0	1.6	0.998	33.4	1.51			
152.6	7.0	46 537	8285	200 000	654.5	3.6	0.975	28.0	2.48			
154.7	10.8	34 830	9240	200 000	632.5		0.970	36.9	1.67			
136.6	17.7	44 140	1660	200 000	651.5		0.920	28.6	1.59			
175.4	14.3	43 180	12 410	200 000	652.6		0.950	29.0	1.77			
70.8	2.7						0.960	19.9	1.05		×	×
98.5	14.1	37 870	394 310	200 000	630.0		0.950	38.5	1.71	×		
117.6	2.9	46 220	3440	200 000	654.3	1.3	0.989	28.0	2.34			
155.4	8.4	39 203	6784	200 000	643.4	3.2	0.929	32.3	2.02			
148.5	4.9	50 971	4915	200 000	652.5	1.7	0.982	29.4	2.19			
217.9	2.9						0.890	38.2	2.32		×	
131.8		77 170		200 000	646.7			34.4	1.46			
111.3	1.9	42 651	2272	200 000	655.6	0.9	0.995	27.1	2.26			
113.6	3.1	70 363	5630	200 000	658.8	1.6	0.993	28.3	2.11			
111.9	3.3	49 541	4072	200 000	640.7	1.8	0.988	34.7	1.96			
195.6	12.8	50 267	10 300	200 000	645.4	3.8	0.932	32.6				
115.9	8.8	50 380	11 400	200 000	632.5	5.9	0.960	38.7				
140.1	5.0	40 041	4393	200 000	632.0	3.2	0.982	37.8				
97.2									2.13			
76.3									1.99			
87.6									1.72			

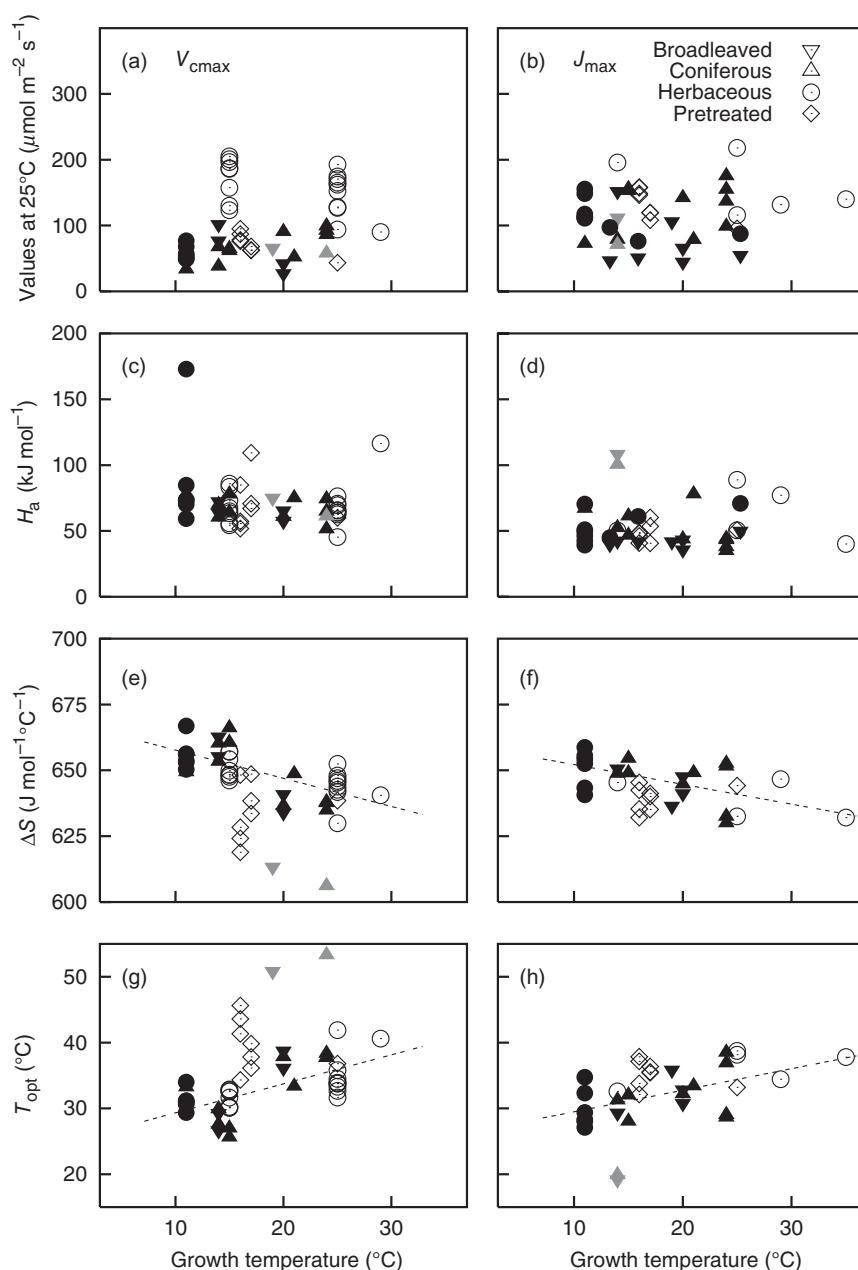


Figure 2. Parameter values of individually fitted functions to characterize the temperature dependence of V_{cmax} (a,c,e,g) and J_{max} (b,d,f,h) in relation to plant growth temperature: (a,b) standard values at 25 °C; (c,d) activation energy (H_a); (e,f) entropy term (ΔS); (g,h) optimum temperature (T_{opt}). Open symbols: plants grown in glasshouses with controlled temperature; closed symbols: plants grown at naturally variable temperature regimes. Linear regressions are shown in dashed lines and are based on all points except when pretreated (rectangles) and those shown in grey [(a,c,e,g): points excluded with optimum temperature above 50 °C; (b,d,h): points excluded with optimum temperature below 20 °C].

significantly, as the slope's 95% confidence interval (twice SE) included zero (Fig. 2a,b, Table 3).

The activation energy, H_a , of V_{cmax} varied from 45 to 90 kJ mol⁻¹ with three outliers above 100 kJ mol⁻¹, and an average of 72 ± 3.3 kJ mol⁻¹ (SE, with an SD of 21 kJ mol⁻¹, see Fig. 2c). The activation energy of J_{max} varied between 35 and 108 kJ mol⁻¹, an average of 50 ± 2.4 kJ mol⁻¹ and an SD of 15 kJ mol⁻¹ (Fig. 2d). The slopes of the temperature accli-

mation functions were slightly negative, but this was again not significant (Table 3). This result was independent of the choice of data, either including or excluding outliers or pretreatment.

The temperature acclimation functions of the entropy terms, ΔS , had negative slopes, -1.07 ± 0.19 J mol⁻¹ K⁻² for V_{cmax} and -0.75 ± 0.21 J mol⁻¹ K⁻² for J_{max} , with an intercept of 668 ± 3.6 and 660 ± 4.1 J mol⁻¹ K⁻¹, respectively

Table 3. Results of linear regression of the form $y = a + bx$ of parameter values (y-value) against growth temperature, (x-value, t_{growth}) and mean values of parameters ['mean(y)']

x-Value	y-Value	x-Min	x-Max	n	Mean(y)	SE	a	SE	b	SE	r^2
t_{growth}	V_{cmax}^{25}	11.0	29.0	44			48.48	29.1	2.78	1.53	0.072
t_{growth}	J_{max}^{25}	11.0	35.0	31			105.77	22.6	0.29	1.18	0.011
t_{growth}	$H_a(V_{\text{cmax}})$	11.0	29.0	38	<u>71 513</u>	3347	82 992	11 360	−632	598	0.030
t_{growth}	$H_a(J_{\text{max}})$	11.0	35.0	24	<u>49 884</u>	2448	53 032	7509	−190	390.2	0.010
t_{growth}	$\Delta S(V_{\text{cmax}})$	11.0	29.0	38	649.12	1.43	<u>668.39</u>	3.64	<u>−1.07</u>	0.19(*)	0.427
t_{growth}	$\Delta S(J_{\text{max}})$	11.0	35.0	24	646.22	1.66	<u>659.70</u>	4.13	<u>−0.75</u>	0.21(*)	0.365
t_{growth}	$T_{\text{opt}}(V_{\text{cmax}})$	11.0	29.0	38	32.92	0.62	24.92	1.60	0.44	0.084(*)	0.433
t_{growth}	$T_{\text{opt}}(J_{\text{max}})$	11.0	35.0	24	32.12	0.67	26.21	1.71	0.33	0.089(*)	0.385
t_{growth}	$r_{\text{J,V}}$	11.0	29.0	28	1.97	0.07	<u>2.59</u>	0.17	<u>−0.035</u>	0.009(*)	0.370

Slopes (b) that are significantly different from 0 are marked by *. Parameter values for the proposed model with temperature acclimation are underlined.

n, number of data points; r^2 , explained variance of y-values; SE, standard error.

(Fig. 2e,f; Table 3). Plants exposed to pretreatment consistently showed a lower ΔS than the respective average without pretreatment (Fig. 2e,f). Assuming a growth temperature of 40 °C, however, which was the temperature during pretreatment which was followed by measurement at 40 °C, would bring them into much better agreement with the other data. The two outliers to lower ΔS in Fig. 2e are related to the data sets with T_{opt} above 50 °C, which had been excluded from the regression analysis of temperature acclimation.

The optimum temperature, T_{opt} , increased by 0.44 ± 0.08 °C for V_{cmax} and 0.33 ± 0.09 °C for J_{max} per 1 °C increase of growth temperature with an intercept of 24.9 ± 1.6 and 26.2 ± 1.7 °C, respectively (Fig. 2g,h; Table 3). As already stated, cases with T_{opt} higher than 50 °C (*Pinus taeda*, *Prunus persica*) or T_{opt} less than 20 °C (*Betula pendula* OTC, *Pinus sylvestris*) were excluded from the regression analysis of temperature acclimation. Including those data would have amplified the observed degree of acclimation of T_{opt} to growth temperature. The impact of growth temperature on T_{opt} in our analysis was caused solely by its effect on ΔS , because H_d was fixed and growth temperature had no significant impact on the activation energy H_a . The T_{opt} of all pretreated plants was above the respective average of plants without pretreatment. Again, assuming a growth temperature of 40 °C, the temperature during pretreatment before measurement at 40 °C would bring those data into much better agreement with the other data.

The optimum temperatures of V_{cmax} and J_{max} were positively correlated, with an r^2 of 0.26 (Fig. 3b). Including the data with pretreatment would increase r^2 to 0.49. This confirms a close coregulation of RuBP carboxylation-limited photosynthesis and RuBP regeneration-limited photosynthesis, even for pretreated plants.

The ratio of J_{max}^{25} to V_{cmax}^{25} , $r_{\text{J,V}}$, depended on plant growth temperature with an intercept of 2.59 ± 0.17 and a slope of -0.035 ± 0.009 K^{−1} (Fig. 3a; Table 3). Without correction for different growth temperatures, J_{max}^{25} and V_{cmax}^{25} were correlated with $r^2 = 0.81$, and an average ratio of 1.97 ± 0.07 (Table 2; Fig. 3c). After correction to a common growth

temperature of 25 °C, r^2 increased to 0.88, while the average ratio decreased to 1.71 ± 0.05 (Fig. 3d). The $r_{\text{J,V}}$ values of pretreated plants are all well below the regression line (Fig. 3a): these plants had grown at 16 °C and 17 °C respectively but they had been pretreated for 1 d at 25 °C before measurement at 25 °C was conducted and may already have acclimated to that temperature, at least to some extent. Assuming a growth temperature of 25 °C, however, would again bring them mostly in line with the other data, in analogy to what was observed for the acclimation of ΔS and T_{opt} . Two data sets showed an exceptionally low value of $r_{\text{J,V}}$: *B. pendula* OTC (1.05) and *P. sylvestris* (1.10) (Fig. 3a). This was caused by their extremely low optimum temperature of J_{max} below 25 °C, while the optimum temperature of V_{cmax} was within the average range and above 25 °C (Fig. 3b). In all other cases, the optimum temperatures of both V_{cmax} and J_{max} were above 25 °C. Therefore, the relationship of J_{max}^{25} to V_{cmax}^{25} seemed to be 'decoupled' in these two cases, and they were hence excluded from the regression analysis of temperature acclimation.

Proposed models with and without acclimation to plant growth temperature

The proposed general model without temperature acclimation is given by Eqn 1 using the following parameter values with uncertainties (averages of the compilation and one SE): 1.97 ± 0.07 for $r_{\text{J,V}}$, 72 ± 3.3 kJ mol^{−1} for H_a and 649 ± 1.43 J mol^{−1} K^{−1} for ΔS of V_{cmax} , 50 ± 2.4 kJ mol^{−1} for H_a and 646 ± 1.66 J mol^{−1} K^{−1} for ΔS of J_{max} (Table 3).

For the general model with temperature acclimation, we propose to include a temperature acclimation of ΔS for V_{cmax} and J_{max} and a temperature acclimation of $r_{\text{J,V}}$, resulting in the following equations:

$$V_{\text{cmax}} = V_{\text{cmax}}^{25} \exp\left[\frac{H_a(T_1 - T_{\text{ref}})}{(T_{\text{ref}}RT_1)}\right] \quad (9)$$

$$1 + \exp\left(\frac{T_{\text{ref}}(a_{\Delta S,V} + b_{\Delta S,V} * t_{\text{growth}}) - H_d}{T_{\text{ref}}R}\right)$$

$$1 + \exp\left(\frac{T_1(a_{\Delta S,V} + b_{\Delta S,V} * t_{\text{growth}}) - H_d}{T_1R}\right)$$

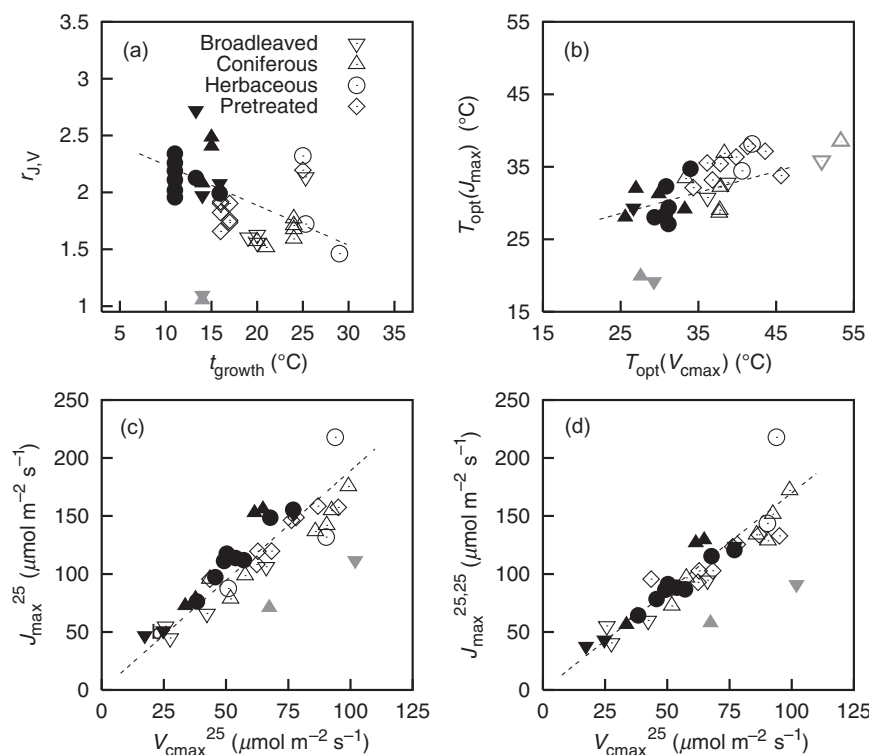


Figure 3. (a) Individually fitted values of the ratio J_{\max}/V_{\max} at standard leaf temperature of 25 °C ($J_{\max}^{25}/V_{\max}^{25} = r_{J,V}$) against growth temperature. (b) Individually fitted optimum temperature of J_{\max} against V_{\max} . (c) J_{\max} against V_{\max} at 25 °C leaf temperature but individual growth temperature. (d) J_{\max} against V_{\max} at 25 °C leaf temperature extrapolated to 25 °C growth temperature using the linear regression shown in (a). Open symbols: plant growth temperature > 18 °C; closed symbols: plant growth temperature < 18 °C. Linear regressions are shown in dashed lines and are based on all points except when pretreated (rectangles) and those shown in grey [(b): points excluded with optimum temperature above 50 °C; (a–d): points excluded with optimum temperature below 20 °C].

$$J_{\max} = (a_{rJ,V} + b_{rJ,V} * t_{\text{growth}}) V_{\max}^{25} \exp[H_a(T_1 - T_{\text{ref}})/(T_{\text{ref}}RT_1)]$$

$$1 + \exp\left(\frac{T_{\text{ref}}(a_{\Delta S,J} + b_{\Delta S,J} * t_{\text{growth}}) - H_d}{T_{\text{ref}}R}\right)$$

$$1 + \exp\left(\frac{T_1(a_{\Delta S,J} + b_{\Delta S,J} * t_{\text{growth}}) - H_d}{T_1R}\right) \quad (10)$$

The base rate, V_{\max}^{25} , still needs to be specified according to species and nutrition, while the activation energy, H_a , is derived as the average from the compilation and is the same as for the model with and without temperature acclimation ($72 \pm 3.3 \text{ kJ mol}^{-1}$ for V_{\max} and $50 \pm 2.4 \text{ kJ mol}^{-1}$ for J_{\max}). The values, a and b , of the temperature regression parameters can be found in Table 3, and the deactivation energy, H_d , is fixed at 200 kJ mol^{-1} .

To evaluate the derived general models with and without temperature acclimation, we compare them against the individually fitted functions, using the RMSE ($RMSE_V$ and $RMSE_J$) as described by Eqns 6 and 8. The individually fitted functions describing V_{\max} , $f_i(T_i)$, show small relative variations below 25 °C and high relative variations above 25 °C (Fig. 4a). Therefore, $RMSE_V$ against the general normalized temperature function without acclimation is small below 25 °C and large above 25 °C (Fig. 4c). Including the temperature acclimation of ΔS (Table 3; Eqn 9) had almost no impact on the temperature dependence of V_{\max} below 25 °C, but the optimum of V_{\max} was shifted to higher temperatures and higher values with increasing plant growth temperatures (Fig. 4e). Accordingly, the temperature acclimation of ΔS did not affect the $RMSE_V$ range below 25 °C, but reduced $RMSE_V$ by up to 25% at temperatures above 25 °C, depending on leaf temperature (Fig. 4g).

For J_{\max} , we show the temperature function $r_{J,V}(T_i)$, which assumes the value of $J_{\max}^{25}/V_{\max}^{25}$ at 25 °C. This ratio varies among the different temperature functions fitted to the individual data sets. As a consequence, the variability between individually fitted functions is relatively high for the whole range of leaf temperatures (Fig. 4b), and $RMSE_J$ against the general normalized temperature function without acclimation is relatively constant (Fig. 4d). J_{\max} normalized to 1 at 25 °C would show a variability similar to V_{\max} . If the general model includes the temperature acclimation of ΔS and $r_{J,V}$ (Table 3; Eqn 10), the optimum of J_{\max} is shifted to higher temperatures with increasing plant growth temperature, but almost constant optimum values (Fig. 4f). Including the temperature acclimation generally reduces the $RMSE_J$ compared to no acclimation for a wide range of leaf temperatures (Fig. 4h).

Impact of temperature acclimation on modelled photosynthesis

Figure 5 presents the impact of the temperature acclimation of V_{\max} and J_{\max} on modelled light-saturated RuBP carboxylation-limited photosynthesis (A_C) and RuBP regeneration-limited photosynthesis (A_J), using the general model with temperature acclimation. Increasing plant growth temperature from 10 to 25 °C shifts the optimum temperature of A_C from about 23 to 29 °C, and the optimum temperature of A_J from about 29 to 33 °C. These results are in good agreement with the optimum temperatures of photosynthesis published by Medlyn *et al.* (2002a). Maximum values of A_C increase, while maximum values of A_J decrease. Both A_C and A_J at low leaf temperatures are

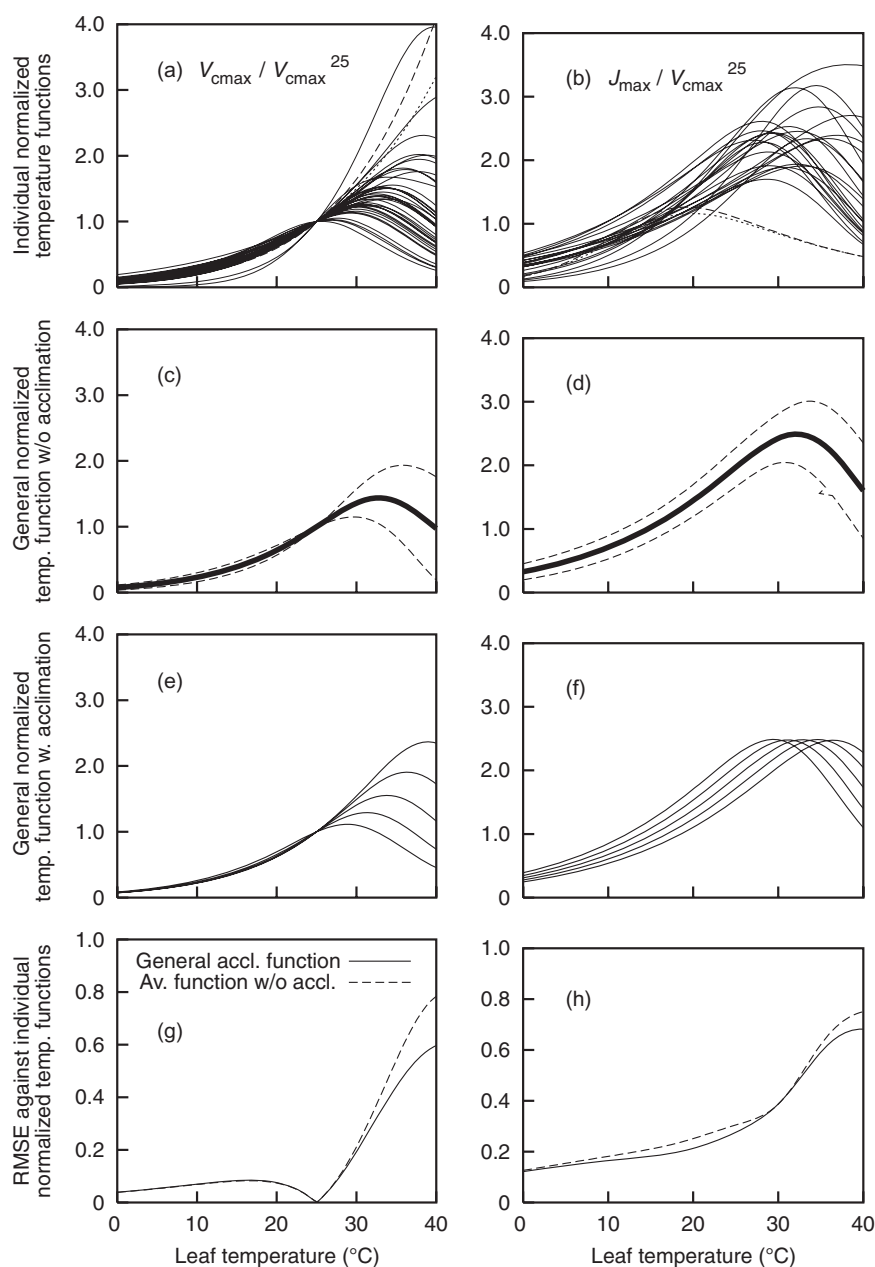


Figure 4. Temperature functions of V_{cmax} (a,c,e) and J_{max} (b,d,f), and root mean square error (RMSE) of general temperature functions against the individually fitted functions (g,h). All curves have been normalized by dividing by the value of V_{cmax} at 25 °C, such that V_{cmax} at 25 °C appears as 1 and J_{max} at 25 °C appears as the ratio of $J_{\text{max}}^{25}/V_{\text{cmax}}^{25}$. (a) Individually fitted temperature functions for V_{cmax} for those data sets which had been used to derive the average models (solid lines). Temperature functions of *Prunus persica* (dashed) and *Pinus taeda* (dotted) with $T_{\text{opt}} > 50$ °C. (b) Same for J_{max} (solid lines), with results for *Betula pendula* OTC (dashed) and *Pinus sylvestris* (dotted) with $T_{\text{opt}} < 20$ °C. (c) General normalized temperature function without temperature acclimation for $V_{\text{cmax}} \pm$ RMSE against the individually fitted functions. (d) The same for J_{max} . (e) General normalized temperature functions with temperature acclimation for V_{cmax} for plant growth temperatures of 10, 15, 20, 25, 30 °C. (f) Same for J_{max} . (g) RMSE for general normalized temperature function with and without temperature acclimation of V_{cmax} against individual fits. (h) Same for J_{max} .

higher for plants grown at 10 °C compared to those grown at 25 °C. For growth temperatures of 10 °C, photosynthesis at light saturation would be limited by A_c at all leaf temperatures, while for a growth temperature of 25 °C, A_j would limit light-saturated photosynthesis at leaf temperatures below 25 °C.

The overall effect of acclimation on gross photosynthesis is summarized in Fig. 5c: plants grown at 10 °C would profit by about 10% at leaf temperatures below 25 °C compared to plants grown at 17 °C, while above 25 °C, modelled photosynthesis would become less effective. Plants grown at 25 °C would have less effective photosynthesis below 25 °C

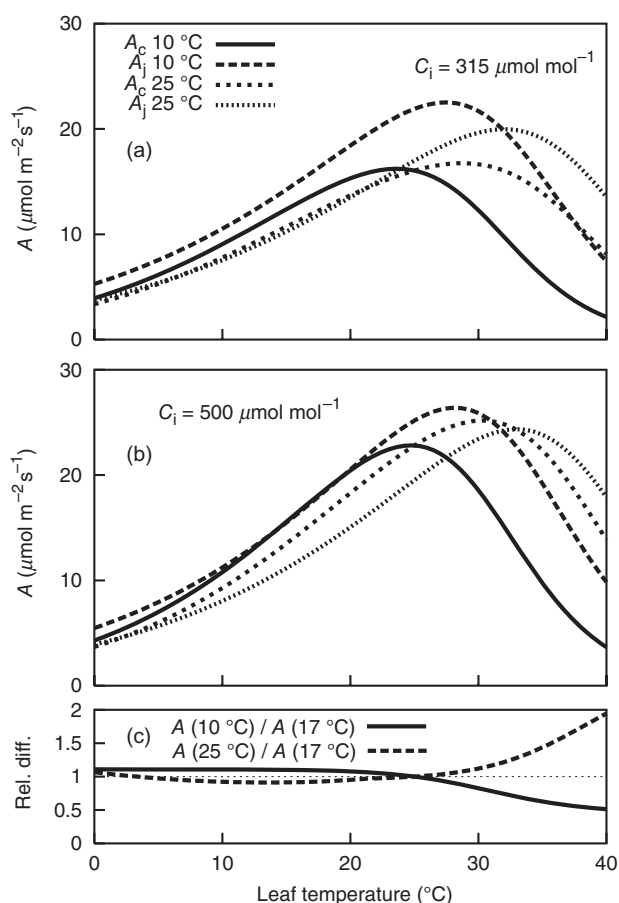


Figure 5. Impact of temperature acclimation on modelled photosynthesis. (a) Light-saturated ribulose-1,5-bisphosphate (RuBP) carboxylation (A_C) and RuBP regeneration (A_J) at intercellular CO_2 concentration (C_i) of 315 ppm (photosynthetically active irradiance = $1500 \mu\text{mol m}^{-2} \text{s}^{-1}$, $V_{\text{cmax}}^{25} = 60 \mu\text{mol m}^{-2} \text{s}^{-1}$). (b) Same as (a) but for C_i of 500 ppm. (c) The ratio of modelled photosynthesis of plants grown at 10 and 25 $^{\circ}\text{C}$ to plants grown at 17 $^{\circ}\text{C}$ for $C_i = 315 \mu\text{mol mol}^{-1}$.

compared to plants grown at 17 $^{\circ}\text{C}$, but above 25 $^{\circ}\text{C}$ photosynthesis would be strongly enhanced, up to as much as 100% at 40 $^{\circ}\text{C}$. Figure 5b shows the combined impact of temperature acclimation and elevated CO_2 on modelled photosynthesis, disregarding the possibility of some CO_2 acclimation happening: A_J would become more limiting, especially for plants grown at high temperatures.

We find that within the relevant ranges of leaf temperature, light-saturated photosynthesis was mostly limited by A_C . The observed temperature acclimation shifted the rates of A_C at optimum temperature to higher values, but interestingly the rates of A_J at optimum temperature decreased. This is caused by the decrease of $r_{J,V}$ with increasing growth temperature. An additional temperature acclimation of V_{cmax}^{25} to higher values at lower growth temperatures would decrease the effect on A_C at T_{opt} , but would further intensify the relative decrease of A_J at T_{opt} with rising growth temperature.

DISCUSSION

Temperature dependence of V_{cmax} and J_{max}

An impact of plant group on the results was only obvious in the case of V_{cmax}^{25} and J_{max}^{25} . Because the photosynthetic capacity, represented by V_{cmax}^{25} and J_{max}^{25} , is related to leaf nitrogen content (Medlyn *et al.* 1999), we assume that this difference is caused by higher leaf nitrogen content and/or a higher nitrogen use efficiency of herbaceous plants compared to trees. An impact of plant group on the activation energy, as observed by Medlyn *et al.* (2002a), was not obvious, except for herbaceous outliers with high values.

An impact of plant growth temperature on V_{cmax}^{25} and J_{max}^{25} could not be observed. Yamori *et al.* (2005) have observed that J_{max}^{25} and V_{cmax}^{25} may increase with decreasing growth temperature to compensate for low values of V_{cmax} and J_{max} at low temperatures. If we assume such an additional acclimation, the increase of V_{cmax}^{25} and J_{max}^{25} for plants grown at low temperatures would further amplify the observed 10% enhancement of photosynthesis at low temperatures for plants acclimated to low temperatures.

In other studies, the activation energy of V_{cmax} and J_{max} has been observed to be positively related to plant growth temperature (Hikosaka *et al.* 1999; Onoda *et al.* 2005). We do not find this acclimation response, and we propose to consider that the reported acclimation response may be an artefact because of the use of the Arrhenius model without modification for a decrease of V_{cmax} and J_{max} at high temperatures, which projects an acclimation of the optimum temperature onto the activation energy.

In case of V_{cmax} , the mismatch between the average normalized function without temperature acclimation and the individually optimized functions (see Eqn 7) was small at temperatures below 25 $^{\circ}\text{C}$ and high at temperatures above 25 $^{\circ}\text{C}$. This is in good agreement with the observation of Leuning (2002). In case of J_{max} , the mismatch was relatively constant for the whole range of leaf temperatures. Including temperature acclimation of ΔS and $r_{J,V}$ substantially reduced the mismatch for V_{cmax} at high temperatures, measured by $RMSE_v$, while the mismatch of J_{max} was only slightly reduced. In general, we find that J_{max} may be well constrained by leaf economy at relatively low temperatures, while at high temperatures it is less constrained, as high temperatures often coincide with high light conditions and photosynthesis is then mostly limited by A_C . Therefore, including the acclimation to plant growth temperature did not substantially reduce $RMSE_J$ at high temperatures.

Outliers in J_{max}^{25} to V_{cmax}^{25} diagram

The ratio of J_{max}^{25} to V_{cmax}^{25} was close to 1.89 apart from two outliers to much lower values, *B. pendula* OTC and *P. sylvestris*. The reason for that was their extremely low optimum temperatures of J_{max} , below the standard temperature of 25 $^{\circ}\text{C}$, while the optimum temperatures of V_{cmax} were above 25 $^{\circ}\text{C}$. Therefore, in these two cases, the standard temperature of 25 $^{\circ}\text{C}$ was on the descending part of the temperature function of J_{max} , while it was on the ascending

part for V_{cmax} . In all other cases, the optimum temperatures of both V_{cmax} and J_{max} were above 25 °C, and the standard temperature of 25 °C was on similar points of the ascending part of the function. It has to be confirmed by further studies, if the two data sets of *B. pendula* OTC and *P. sylvestris*, which are the only ones from the boreal area, are indeed outliers with respect to the optimum temperature of J_{max} and the ratio of $J_{\text{max}}^{25}/V_{\text{cmax}}^{25}$, or if they are representative for boreal plants.

Application in large-scale models

Even the moderate acclimation response of V_{cmax} and J_{max} derived within this study would have a considerable effect on modelled photosynthesis rates, especially at high temperatures. This effect of acclimation on modelled photosynthesis would be highly relevant for a use within climate predictions, as the effect of the expected temperature increase on the terrestrial biosphere is not only significant for cold areas, as has been assumed in earlier predictions, but also for tropical areas (Cox *et al.* 2004; Raddatz *et al.* 2007).

A recent comparison of scenarios of coupled climate and terrestrial biosphere models for the next 100 years showed an increase of average global temperatures between 1.5 and 4 °C with CO₂ concentrations rising to between 800 and 1000 ppm (Friedlingstein *et al.* 2006). The temperature increase can be expected to vary considerably between different regions, rising by up to 10 °C in the Amazon basin (Raddatz *et al.* 2007), where average daily maximum temperatures already exceed 33 °C, and daily averages are about 27 °C. It will be crucial to understand, to which extent the vegetation in these already hot areas will be able to adapt to climate changes, either by acclimation or by migration. An acclimation of photosynthesis to these temperature ranges is physiologically not impossible. The temperature optimum of photosynthesis of the desert plant *Tidestromia oblongifolia*, for example, is close to 50 °C (Berry & Raison 1981). But an acclimation to extreme temperatures is a property that is specific for the different species. Therefore, a considerable change of species composition can be expected.

When modelling the terrestrial carbon balance, not only the temperature acclimation of photosynthesis has to be taken into account, but also possible acclimation effects on plant and soil respiration, which could significantly affect the temperature optimum of net photosynthesis and the long-term carbon balance of ecosystems (Luo *et al.* 2001; Atkin *et al.* 2005). While observations of apparent temperature acclimation of soil respiration can be fully explained by Arrhenius kinetics without the need for any biological adaptation mechanism (Knorr *et al.* 2005), the temperature acclimation of plant respiration needs better process-based understanding to be quantified (Atkin *et al.* 2005). However, in case of this reanalysis, any temperature acclimation of respiration is implicitly taken into account as leaf respiration is simultaneously obtained from the gas exchange measurements and subtracted before estimating V_{cmax} and J_{max} .

Which is the relevant time-scale of a temperature acclimation for V_{cmax} and J_{max} if we want to model ecosystem carbon fluxes? Here, we haven chosen a period of about 1 month, because Medlyn *et al.* (2002b) concluded from a case study on *Pinus pinaster* that the short-term temperature response of photosynthesis varies on a seasonal basis. In one case, however, they also observed a faster response of the optimum temperature of J_{max} , but not consistently. Yamori *et al.* (2005, 2006) analysed the acclimation of photosynthetic metabolism to a transfer from high to low plant growth temperatures for spinach. Measurements started 2 weeks after the transfer. RuBP regeneration was already almost identical compared to plants that had continuously grown at low temperatures. An acclimation of RuBP carboxylation was also obvious and ascribed to Rubisco kinetics and Rubisco activation state. In our reanalysis, a partial temperature acclimation of V_{cmax} and J_{max} was already likely after continuous pretreatment of only 24 h at constant temperature. Therefore, we must consider that temperature acclimation of V_{cmax} and J_{max} may not only be relevant for long-term predictions or seasonal time-scales, but a partial acclimation to average temperature experienced over time-scales of days may already be relevant for modelled photosynthetic rates. Carefully designed experiments will be necessary to fully determine to which degree temperature acclimation occurs at submonthly down to daily time-scales. Likewise, we suggest that adequately designed modelling studies will be used to determine the possible impact of shorter-term temperature acclimation on simulated carbon fluxes.

CONCLUSIONS

This compilation contains data from 36 species including herbaceous plants, broadleaved trees and coniferous trees. Compared to the compilation by Medlyn *et al.* (2002a), it includes more and several newer data sets. Because some important groups are still missing, such as tropical trees, or are not well represented, as boreal trees, the results still need to be validated for those cases. Nevertheless, the results of this study indicate a general tendency for an acclimation response of V_{cmax} and J_{max} to plant growth temperature, which is derived from experimental data on a large number of species and experiments. The resulting generalized formulation should therefore be suitable for use in global carbon cycle and climate modelling studies.

ACKNOWLEDGMENTS

We would like to very much thank Christian Wirth, three anonymous reviewers and the subject editor, Steve Long, for helpful comments on the manuscript. This work has been financed and supported by the European Union (EU) project CAMELS, contract number EVK2-CT-2002-00151, within the EU's fifth framework program for Research and Development, the Max-Planck-Gesellschaft zur Förderung der Wissenschaften e.V. and the Natural Environment Research Council under QUEST.

REFERENCES

- Atkin O.K., Bruhn D., Hurry V.M. & Tjoelker M.G. (2005) The hot and the cold: unravelling the variable response of plant respiration to temperature. *Functional Plant Biology* **32**, 87–105.
- Bernacchi C.J., Singaas E.L., Pimentel C., Portis A.R. & Long S.P. (2001) Improved temperature response functions for models of Rubisco-limited photosynthesis. *Plant, Cell & Environment* **24**, 253–259.
- Bernacchi C.J., Pimentel C. & Long S.P. (2003) *In vivo* temperature response functions of parameters required to model RuBP-limited photosynthesis. *Plant, Cell & Environment* **26**, 1419–1430.
- Berry J.A. & Raison J.K. (1981) Response of macrophytes to temperature. In *Encyclopedia of Plant Physiology* (eds O.L. Lange, P.S. Nobel, C.B. Osmond & H. Ziegler), pp. 277–338. Springer, Berlin, Germany.
- Braswell B.H., Sacks W.J., Linder E. & Schimel D.S. (2005) Estimating diurnal to annual ecosystem parameters by synthesis of a carbon flux model with eddy covariance net ecosystem exchange observations. *Global Change Biology* **11**, 335–355.
- Bunce J.A. (2000) Acclimation of photosynthesis to temperature in eight cool and warm climate herbaceous C₃ species: temperature dependence of parameters of a biochemical photosynthesis model. *Photosynthesis Research* **63**, 59–67.
- von Caemmerer S. (2000) *Biochemical Models of Leaf Photosynthesis*. CSIRO Publishing, Canberra, Australia.
- Cox P.M., Betts R.A., Jones C.D., Spall S.A. & Totterdell I.J. (2000) Acceleration of global warming due to carbon-cycle feedbacks in a coupled climate model. *Nature* **408**, 184–187.
- Cox P.M., Betts R.A., Collins M., Harris P.P., Huntingford C. & Jones C.D. (2004) Amazonian forest dieback under climate-carbon cycle projections for the 21st century. *Theoretical and Applied Climatology* **78**, 137–156.
- Dreyer E., Le Roux X., Montpied P., Daudet F.A. & Masson F. (2001) Temperature response of leaf photosynthetic capacity in seedlings from seven temperate tree species. *Tree Physiology* **21**, 223–232.
- Dungan R.J., Whitehead D. & Duncan R.P. (2003) Seasonal and temperature dependence of photosynthesis and respiration for two co-occurring broad-leaved tree species with contrasting leaf phenology. *Tree Physiology* **23**, 561–568.
- Farquhar G.D., von Caemmerer S. & Berry J.A. (1980) A biochemical model of photosynthetic CO₂ assimilation in leaves of C₃ species. *Planta* **149**, 78–90.
- Friedlingstein P., Cox P., Betts R., et al. (2006) Climate-carbon cycle feedback analysis, results from the C4MIP model intercomparison. *Journal of Climate* **19**, 3337–3353.
- Han Q.M., Kawasaki T., Nakano T. & Chiba Y. (2004) Spatial and seasonal variability of temperature responses of biochemical photosynthesis parameters and leaf nitrogen content within a *Pinus densiflora* crown. *Tree Physiology* **24**, 737–744.
- Harley P.C., Thomas R.B., Reynolds J.F. & Strain B.R. (1992) Modelling photosynthesis of cotton grown in elevated CO₂. *Plant, Cell & Environment* **15**, 271–282.
- Harley P.C., Weber J.A. & Gates D.M. (1985) Interactive effects of light, leaf temperature, CO₂ and O₂ on photosynthesis in soybean. *Planta* **165**, 249–263.
- Hikosaka K., Murakami A. & Hirose T. (1999) Balancing carboxylation and regeneration of ribulose-1,5-bisphosphate in leaf photosynthesis: temperature acclimation of an evergreen tree, *Quercus myrsinifolia*. *Plant, Cell & Environment* **22**, 841–849.
- Johnson F., Eyring H. & Williams R. (1942) The nature of enzyme inhibitions in bacterial luminescence: sulphanilamide, urethane, temperature, pressure. *Journal of Cell Comparative Physiology* **20**, 247–248.
- Kirschbaum M.U.F. & Farquhar G.D. (1984) Temperature dependence of whole-leaf photosynthesis in *Eucalyptus pauciflora* Sieb. ex Spreng. *Australian Journal of Plant Physiology* **11**, 519–538.
- Knorr W. & Kattge J. (2005) Inversion of terrestrial ecosystem model parameter values against eddy covariance measurements by Monte Carlo sampling. *Global Change Biology* **11**, 1333–1351.
- Knorr W., Prentice I.C., House J.I. & Holland E.A. (2005) Long-term sensitivity of soil carbon turnover to warming. *Nature* **433**, 298–301.
- Leuning R. (1997) Scaling to a common temperature improves the correlation between photosynthesis parameters J_{\max} and V_{\max} . *Journal of Experimental Botany* **307**, 345–347.
- Leuning R. (2002) Temperature dependence of two parameters in a photosynthesis model. *Plant, Cell & Environment* **25**, 1205–1210.
- Levenberg K. (1944) A method for the solution of certain problems in least squares. *Quarterly of Applied Mathematics* **2**, 164–168.
- Luo Y.Q., Wan S.Q., Hui D.F. & Wallace L.L. (2001) Acclimatization of soil respiration to warming in a tall grass prairie. *Nature* **413**, 622–625.
- Medlyn B.E., Badeck F.W., Pury D.G.G.D., et al. (1999) Effects of elevated CO₂ on photosynthesis in European forest species: a meta-analysis of model parameters. *Plant, Cell & Environment* **22**, 1475–1495.
- Medlyn B.E., Dreyer E., Ellsworth D., et al. (2002a) Temperature response of parameters of a biochemically based model of photosynthesis. II. A review of experimental data. *Plant, Cell & Environment* **25**, 1167–1179.
- Medlyn B.E., Loustau D. & Delzon S. (2002b) Temperature response of parameters of a biochemically based model of photosynthesis. I. Seasonal changes in mature maritime pine (*Pinus pinaster* Ait.). *Plant, Cell & Environment* **25**, 1155–1165.
- Misson L., Tu K.P., Boniello R.A. & Goldstein A.H. (2006) Seasonality of photosynthetic parameters in a multi-specific and vertically complex forest ecosystem in the Sierra Nevada of California. *Tree Physiology* **26**, 729–741.
- Onoda Y., Hikosaka K. & Hirose T. (2005) The balance between RuBP carboxylation and RuBP regeneration: a mechanism underlying the interspecific variation in acclimation of photosynthesis to seasonal change in temperature. *Functional Plant Biology* **32**, 903–910.
- Raddatz T., Reick C., Knorr W., Kattge J., Roeckner E., Schnur R., Schnitzler K.-G., Wetzell P. & Jungclaus J. (2007) Will the tropical land biosphere dominate the climate-carbon cycle feedback during the 21st century? *Climate Dynamics*. doi: 10.1007/s00382-007-0247-8.
- Robakowski P., Montpied P. & Dreyer E. (2002) Temperature response of photosynthesis of silver fir (*Abies alba* Mill.) seedlings. *Annals of Forest Science* **59**, 159–166.
- Strassmeyer J. & Forstreuter M. (1997) Parameterization of a leaf gas-exchange model for *Fagus sylvatica* L. using microcosms grown under ambient and elevated CO₂. *Landschaftsentwicklung und Umweltforschung* **107**, 61–72.
- Walcroft A.S. & Kelliher F.M. (1997) The response of photosynthetic model parameters to temperature and nitrogen concentration in *Pinus radiata* D. Don. *Plant, Cell & Environment* **20**, 1338–1348.
- Walcroft A., Le Roux X., Diaz-Espejo A., Dones N. & Sinoquet H. (2002) Effects of crown development on leaf irradiance, leaf morphology and photosynthetic capacity in a peach tree. *Tree Physiology* **22**, 929–938.
- Wang K.Y., Kellomaki S. & Laitinen K. (1996) Acclimation of photosynthetic parameters in Scots pine after three years exposure to elevated temperature and CO₂. *Agricultural and Forest Meteorology* **82**, 195–217.

- Wang Y.P., Leuning R., Cleugh H.A. & Coppin P.A. (2001) Parameter estimation in surface exchange models using nonlinear inversion: how many parameters can we estimate and which measurements are most useful? *Global Change Biology* **7**, 495–510.
- Wang Y.P., Baldocchi D., Leuning R., Falge E. & Vesala T. (2007) Estimating parameters in a land-surface model by applying nonlinear inversion to eddy covariance flux measurements from eight FLUXNET sites. *Global Change Biology* **13**, 652–670.
- Wilson K.B., Baldocchi D.D. & Hanson P.J. (2000) Spatial and seasonal variability of photosynthetic parameters and their relationship to leaf nitrogen in a deciduous forest. *Tree Physiology* **20**, 565–578.
- Wohlfahrt G., Bahn M., Haubner E., Horak I., Michaeler W., Rottmar K., Tappeiner U. & Cernusca A. (1999) Inter-specific variation of the biochemical limitation to photosynthesis and related leaf traits of 30 species from mountain grassland ecosystems under different land use. *Plant, Cell & Environment* **22**, 1281–1296.
- Wullschlegel S.D. (1993) Biochemical limitations to carbon assimilation in C₃ plants – a retrospective analysis of the A/C_i curves from 109 species. *Journal of Experimental Botany* **44**, 907–920.
- Yamori W., Noguchi K. & Terashima I. (2005) Temperature acclimation of photosynthesis in spinach leaves: analyses of photosynthetic components and temperature dependencies of photosynthetic partial reactions. *Plant, Cell & Environment* **28**, 536–547.
- Yamori W., Suzuki K., Noguchi K., Nakai M. & Terashima I. (2006) Effects of Rubisco kinetics and Rubisco activation state on the temperature dependence of the photosynthetic rate in spinach leaves from contrasting growth temperatures. *Plant, Cell & Environment* **29**, 1659–1670.

Received 30 November 2006; received in revised form 4 May 2007; accepted for publication 7 May 2007